




Short Note

Paenidigyamycin G: 1-Acetyl-2,4-dimethyl-3-phenethyl-1*H*-imidazol-3-ium

Gilbert Mawuli Tetevi ¹, Samuel Kwain ¹, Thomas Mensah ¹, Anil Sazak Camas ²,
Mustafa Camas ² , Aboagye Kwarteng Dofuor ³, Faustus Akankperiwen Azerigyik ⁴,
Emmanuel Oluwabusola ⁵, Hai Deng ⁵ , Marcel Jaspars ⁵ and Kwaku Kyeremeh ^{1,*} 

¹ Marine and Plant Research Laboratory of Ghana, Department of Chemistry, School of Physical and Mathematical Sciences, University of Ghana, P.O. Box LG 56, Legon-Accra, Ghana; gilberttet@gmail.com (G.M.T.); kwainsamuel75@gmail.com (S.K.); tmensah012@st.ug.edu.gh (T.M.)

² Department of Bioengineering, Munzur University, Tunceli 62000, Turkey; anilsazak@gmail.com (A.S.C.); mustafacamas@gmail.com (M.C.)

³ Department of Biochemistry, Cell and Molecular Biology, University of Ghana, P.O. Box LG 54, Legon-Accra, Ghana; akwartengdofuor@yahoo.com

⁴ Noguchi Memorial Institute for Medical Research (NMIMR), College of Health Sciences, University of Ghana, P.O. Box LG 581, Legon-Accra, Ghana; faustusazerigyik@gmail.com

⁵ Marine Biodiscovery Centre, Department of Chemistry, University of Aberdeen, Old Aberdeen AB24 3UE, Scotland, UK; r01eto16@abdn.ac.uk (E.O.); h.deng@abdn.ac.uk (H.D.); m.jaspars@abdn.ac.uk (M.J.)

* Correspondence: kkyeremeh@ug.edu.gh; Tel.: +233-20-789-1320

Received: 20 October 2019; Accepted: 11 November 2019; Published: 21 November 2019



Abstract: The Ghanaian *Paenibacillus* sp. DE2SH (GenBank Accession Number: MH091697) is a prolific producer of potent antiparasitic alkaloids. Further detailed study of the culture broth of this strain produced the compound Paenidigyamycin G (**1**), which is a derivative of the known antiparasitic compound Paenidigyamycin A (**2**). Compound (**1**) was isolated on HPLC at $t_R \approx 37.5$ min and its structure determined by IR, UV, MS, 1D, and 2D-NMR data. Compound **1** produced weak to moderate antileishmanial and antitrypanosomal activity when tested against *Leishmania donovani* (Laveran and Mesnil) Ross (D10) and *Trypanosoma brucei* subsp. *brucei* strain GUTat 3.1 with $IC_{50} = 115.41$ and $28.75 \mu M$, respectively. This result is interesting since the parent compound **2** is known to possess consistent and potent antiparasitic activity. However, **1** displayed a promising selectivity profile towards *T. brucei* subsp. *brucei* due to its relatively low toxicity against normal mouse macrophages RAW 264.7 cells ($SI = 8.70$). Given that compound **1** is also the main metabolite found in the hexane fraction of all extracts produced by *Paenibacillus* sp. DE2SH when it is co-cultured with other bacteria strains, it must possess some unique biological functions which should make it an excellent candidate for further biological activity screening in other bioassays.

Keywords: Paenibacillus; alkaloid; imidazole; antileishmanials; leishmaniasis; antitrypanosomals; trypanosomiasis

1. Introduction

Schistosomiasis, leishmaniasis, and human African trypanosomiasis (HAT) are common neglected parasitic infections that affect people in sub-Saharan Africa (SSA) and together produce a huge disease burden in the region [1–3]. It is estimated that for schistosomiasis alone, over 200 million infection cases and 280,000 schistosomiasis-related deaths are recorded yearly, the majority of which can be found in SSA [4]. Also, the World Health Organization (WHO) comprehensive statistics on leishmaniasis shows that an estimated 1 million new cases of this infection are recorded each year with significantly rising

levels of the deadly visceral leishmaniasis [5]. Comparatively, infection figures for HAT in SSA have dwindled over the past decade but, nevertheless, a lot more needs to be accomplished to prevent a huge resurgence of the disease and treatment for the millions of people who continue to harbor the parasite [6].

While these disabling, chronic, and very painful illnesses occur mostly in the settings of extreme poverty, their troubling socio-economic impacts also remains the case why these poor populations of SSA may not be able to escape poverty [7,8]. Unfortunately, current available antiparasitic drugs for the treatment of schistosomiasis, leishmaniasis, and HAT have severe limitations. Factors such as widespread development of drug resistance, undesirable and sometimes fatal side effects, complicated and long drug administration procedures, and high toxicity profiles associated with the current drugs have made them less appreciable for treatment [9–11]. The main goal of most stakeholders, especially those of endemic countries, is to greatly reduce the disease burden of schistosomiasis, leishmaniasis, and HAT [12,13]. However, it is evident that without the availability of chemical structure diversity and effective drugs to treat all developmental stages of these parasitic infections, efforts to reduce the burden of these diseases will be significantly hampered. It is therefore urgent that new and robust antiparasitic drugs are continually discovered and developed as part of efforts to control, cure, and eradicate parasitic neglected tropical diseases.

In recent years, imidazole-associated natural products have gained significant scientific exploration for possible antiparasitic drug development [14]. The imidazole nucleus represents an important heterocyclic core in several biologically active compounds [15,16] and has been found to exhibit unique medicinal properties such as; excellent tissue penetrability and permeability, high bioavailability and low incidence of adverse toxicity [17]. Imidazole-associated natural products as well as their synthetic derivatives are known to demonstrate a wide spectrum of biological activities including: capravirine (antiviral) [17], metronidazole (antimicrobial) [18], futrimazole (antifungal) [19], losartan (cardiovascular) [20], flumizole (anti-inflammatory) [21], nafimidone (anticonvulsant) [22], cimetidine (anticancer agents) [23], and paenidigyamycin A (antiparasitic) [24]. Many imidazole-based compounds have very useful clinical applications. A critical look at the structures of some of the imidazole-based compounds mentioned herein reveal a wide diversity of structural modifications that can exist on the imidazole scaffold and how these substitutions are crucial to the medicinal properties and the biological potency exerted by imidazole compounds.

In the last four years, we have collected several soils and sediments from extreme biodiverse environments in Ghana, especially, wetlands from the western and Brong Ahafo regions. Several cultivable microbial strains were isolated from these samples. Initial biological investigation of the extracts of the strains yielded promising antiparasitic activities. In an earlier report, we described the detection, isolation, and characterization of Paenidigyamycin A (**2**) (Figure S12), a potent antiparasitic imidazole alkaloid from the Ghanaian *Paenibacillus* sp. DE2SH [24]. Compound **2**, a dimer of the imidazole nucleus was tested against a variety of parasites and was found to consistently exert potent antileishmanial activity against *L. major* (IC₅₀ 0.75 μM) and *L. donovani* (IC₅₀ 7.02 μM). Compound **2** also exhibited strong antitrypanosomal activity against *T. brucei* subsp. *brucei* strain GUTat 3.1 (IC₅₀ 0.78 μM).

Herein, we report on the isolation and characterization of 1-acetyl-2,4-dimethyl-3-phenethyl-1*H*-imidazol-3-ium or simply Paenidigyamycin G (**1**) which is a derivative of the imidazole alkaloid **2** (Figure 1). Fractionation of the crude extracts of the *Paenibacillus* sp. strain DE2SH through solvent partitioning by a modification of Kupchan's method [25] gave four fractions; hexane (FH), dichloromethane (FD), methanol/water (FM), and butanol/water (WB). Chemical profiling of the Kupchan sub-fractions using high resolution electrospray ionization liquid chromatography mass spectrometry (HRESI-LC-MS) and nuclear magnetic resonance spectroscopy (NMR) coupled with phytochemical screening on thin-layer chromatography (TLC) plates using Dragendorff and Ninhydrin reagents showed the FH to contain an alkaloid which was structurally related to **2**. Coincidentally, this alkaloid was the major metabolite also seen in the FH fractions whenever strain DE2SH was

co-cultured with other microbial strains. Therefore, the FH fraction was subjected to reverse phase HPLC which yielded Paenidigyamycin G (**1**) at a concentration of 1.3 mg/L.

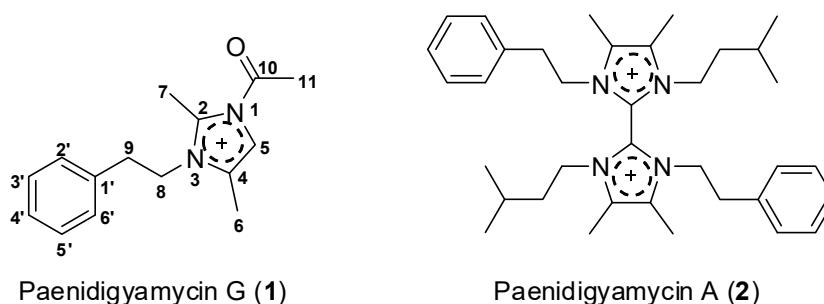


Figure 1. Structure of Paenidigyamycin G: 1-acetyl-2,4-dimethyl-3-phenethyl-1H-imidazol-3-ium (**1**) and Paenidigyamycin A (**2**).

2. Results

2.1. Sediment Sample Collection Sites

Details of the soil and sediment sample collection sites and GPS coordinates can be found in an article we have already published [24].

2.2. Taxonomy of Strain DE2SH

The taxonomy of the Ghanaian *Paenibacillus* sp. strain DE2SH (GenBank Accession Number: MH091697) has been described in a previous publication [24].

2.3. Structure Determination of Paenidigyamycin G (**1**)

Compound **1** was obtained by semi-preparative reverse phase HPLC at t_R of 37.5 min (Figure S1) as a light yellow oil when completely free of solvent. The HRESI-LC-MS of compound **1** gave m/z of 243.1565, corresponding to a molecular formula of $C_{15}H_{19}N_2O^+$ ($\Delta = 0.01$ and 8 degrees of unsaturation). From this ion, a characteristic loss of an acetyl group produced m/z 200.1424 corresponding to molecular formulas $C_{13}H_{16}N_2^{+}$ ($\Delta = 0.01$ ppm and 7 degrees of unsaturation). Other classical fragmentation patterns leading to different ions can be found in Figure S3. Analysis of the 1H , ^{13}C , and multiplicity edited pulsed field gradient heteronuclear single quantum coherence (gHSQCAD) and several pulsed field gradient 1H - ^{13}C heteronuclear multiple bond correlations (gHMBCAD) spectra of **1**, suggested the presence of 4 quaternary, 6 methine, 2 methylene, and 3 methyl carbons. The presence of a mono-substituted benzene ring was easily identified by the 1H -NMR chemical shifts δ_H 7.09 (2H, m, H-2', H-6'), 7.20 (1H, m, H-4'), and 7.25 (2H, m, H-3', H-5'). Detailed analysis of the 1H - 1H homonuclear correlation spectroscopy (gCOSY) spectrum showed correlations H-2'/H-3' and H-5'/H-6', which were further corroborated by similar 1H - 1H total correlation spectroscopy (2D-TOCSY) correlations, including H-2'/H-4', H-6'/H-4', H-3'/H-4', and H-5'/H-4' to fully establish this aromatic spin system. The gHMBCAD correlations C-1' to H-8, and C-1' to H-9, showed that the aromatic system was attached to an ethyl group with carbon atoms at δ_C 47.0 (C-8) and 36.9 (C-9) and δ_H 4.48 (2H, t, $J = 7.2$ Hz, H-8) and 2.92 (2H, t, $J = 7.2$ Hz, H-9), respectively. The gCOSY correlations H-8/H-9 and H-8'/H-9' confirmed this isolated spin system with the lower methylene chemical shift carbon δ_C 36.9 (C-9) attached to the mono-substituted benzene ring; while the higher methylene chemical shift carbon δ_C 47.0 (C-8) was attached to a nitrogen of possible heteroaromatic system. Further confirmation of this structure was provided by the HRESI-LC-MS data of **1** (Figure S3), which showed a peak at m/z 105.0690 corresponding to $C_8H_9^+$ ($\Delta = 0.001$ ppm and 4 degrees of unsaturation). The presence of the carbons δ_C 137.3 (C-2), 122.3 (C-4), 116.5 (C-5), 9.7 (C-6), and 8.2 (C-7) were characteristic and suggested the presence of two methyl substituents on an imidazole ring. The gHMBCAD correlations H-5 to C-2, C-4 and C-6, H-6 to C-4, C-5 and C-2, H-7 to C-4 and C-2, H-8 to C-2 and C-9 further confirmed

the attachment of imidazole nitrogen to a phenethyl moiety and also the positions of attachment of two methyl carbons to the imidazole ring. Taking the current substructures forward for the full structure determination, an acetyl moiety was identified with δ_C 187.5 (C-10) and 25.4 (C-11), which was confirmed by the gHMBCAD correlation H-11 to C-10.

Due to the lack of clear spin systems within the imidazole backbone, the ^1H - ^1H rotating-frame Overhauser spectroscopy (ROESY) data was crucial to facilitate the correct placements of substituents around the imidazole ring. The ROESY correlations used to finalize the structure include: H-5/H-11, H-8/H-2', H-6' and H-9, H-9/H-2', H-6' and H-8. These ROESY correlations in addition to all the other pieces of data facilitated the placement of the acetyl moiety at N-1.

The complete NMR data for Compound 1 is given in Table 1 while the raw data can be found in the Supplementary Figures S4–11. In Figures 2 and 3, a visual representation of COSY, HMBC, 2D-TOCSY, and ROESY correlations are shown.

Table 1. 1D and 2D-NMR spectroscopic data for compound (1) in CD_3OD , in ppm.

#	δ_C mult	δ_H mult (J Hz)	^1H - ^1H COSY	HMBC	TOCSY
1-N					
2	137.3, C				
3-N					
4	116.5, C				
5	122.3, CH	6.96, s	6	C-2, C-4, C-6	
6	9.7, CH ₃	1.99, s	5	C-4, C-5, C-2	
7	8.2, CH ₃	1.90, s		C-4, C-2	
8	47.0, CH ₂	4.48, t (7.2)	9	C-2, C-9	9
9	36.9, CH ₂	2.92, t (7.2)	2', 8	C-2', C-1', C-8	8
10	187.5, C				
11	25.4, CH ₃	2.39, s		C-10	
1'	138.7, C				
2'	128.7, CH	7.09, m	3', 9	C-4', C-6', C-9	3'
3'	128.0, CH	7.25, m	2'	C-5', C-1'	2', 6'
4'	126.0, CH	7.20, m			3', 2', 6'
5'	128.0, CH	7.25, m	2'	C-3', C-1'	2', 6'
6'	128.7, CH	7.09, m	3'	C-4', C-2', C-9	3'

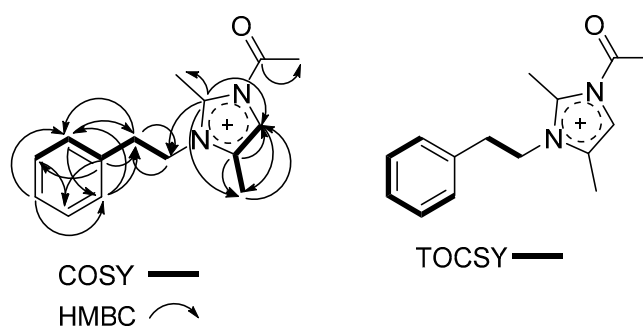


Figure 2. Key COSY (bold lines), ^{13}C - ^1H HMBC (single arrows), and TOCSY (bold lines) correlations for compound 1.

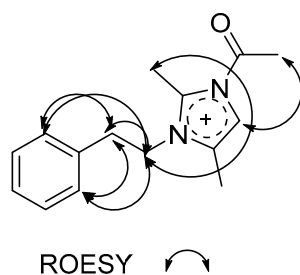


Figure 3. Key ROESY (double arrow) correlations for compound **1**.

Due to the potent antiparasitic activity shown previously by the parent compound paenidigyamycin A (**2**), **1** was also tested for antiparasitic activity against trypanosome and leishmania parasites. However, **1** was found to exhibit moderate to weak antiparasitic activity against these parasites. For both *T. brucei brucei* and *L. donovani* cells, **1** was observed to be far less potent compared to **2** which demonstrated very potent antitrypanosomal and antileishmanial activities. The laboratory standards used for the antitrypanosomal and antileishmanial assays were diminazene aceturate (IC_{50} 1.86 μ M) and amphotericin B (IC_{50} 0.33 μ M) respectively. However, in the presence of mouse macrophages RAW 264.7 cell lines, compound **1** was found to display relatively low toxicity profile on *T. brucei brucei* with selectivity index (SI) of 8.70 (Figure 4). These results suggest that **1** is relatively non-toxic to normal cells and if found active in other bioassay screens, would exhibit interesting bioactivity.

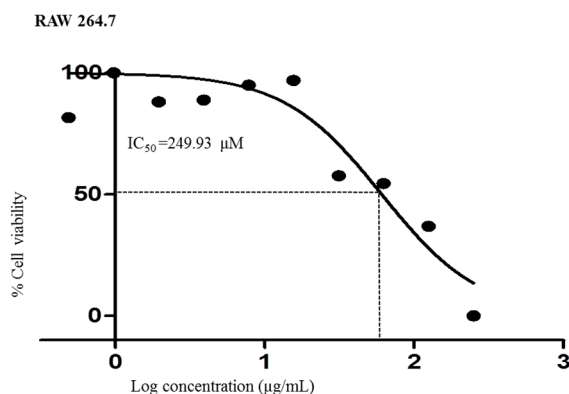


Figure 4. Dose-response curve for compound **1**: IC_{50} value was calculated from the cell viability analysis in normal mouse macrophages (RAW 264.7). A selectivity index (SI) of 8.70 was obtained by calculating the ratio of the IC_{50} in RAW 264.7 cells to that in *T. brucei brucei* cells.

3. Experimental Section

3.1. General Experimental Procedures

1D and 2D NMR data were recorded on a Bruker AVANCE III HD Prodigy (BRUKER, Sylvenstein, Germany) at 500 and 125 MHz for 1H and ^{13}C , respectively. This instrument was optimized for 1H observation with pulsing/decoupling of ^{13}C and ^{15}N , with 2H lock channels equipped with shielded z-gradients and cooled preamplifiers for 1H and ^{13}C . The 1H and ^{13}C chemical shifts were referenced to the solvent signals (δ_H 3.31 ppm and δ_C 49.00 ppm in CD_3OD). High-resolution mass spectrometry data were measured using a ThermoScientific LTQXL-Discovery Orbitrap (Thermo Scientific, Bremen, Germany) coupled to an Accela UPLC-DAD system. The following conditions were used for mass spectrometric analysis: capillary voltage 45 V, capillary temperature 320 $^{\circ}C$, auxiliary gas flow rate 10–20 arbitrary units, sheath gas flow rate 40–50 arbitrary units, spray voltage 4.5 kV, and mass range 100–2000 amu (maximum resolution 30,000). Semi-preparative HPLC purifications were carried out using a Phenomenex Luna reverse-phase (C18 250 \times 10 mm, L \times i.d.) column connected to a Waters

1525 Binary HPLC pump Chromatograph with a 2998 photodiode array detector (PDA), column heater, and in-line degasser. Detection was achieved on-line through a scan of wavelengths from 200 to 400 nm. This system was also used to record the UV profile for the compound. IR was measured using a PerkinElmer FT-IR (UATR Two) spectrometer. All solvents were HPLC grade. Sephadex LH-20 and HP-20 resin were obtained from Sigma Aldrich (Munich, Germany).

3.2. Isolation and Purification of the *Paenibacillus* sp. Strain DE2SH

Isolation, purification, identification, and laboratory cultivation of the Ghanaian *Paenibacillus* sp. DE2SH were previously described by our group [24].

3.3. Fermentation of *Paenibacillus* sp. Strain DE2SH

Autoclaved Erlenmeyer flask (250 mL) plugged with non-absorbent cotton wool containing 50 mL of TSBY (5 g of tryptic soy, 0.3 g of yeast, and 2 g of sucrose) fermentation media in distilled water was directly inoculated with spores of strain DE2SH and incubated at 28 °C at 220 rpm for 3 days. This seed culture was subsequently used to inoculate nine autoclaved 1 L Erlenmeyer flasks each containing 200 mL TSBY (20 g of tryptic soy, 1 g of yeast, and 6 g of sucrose) fermentation media and plugged with non-absorbent cotton wool. The 1 L flasks were incubated at 28 °C at 220 rpm for 14 days. Two days before the culture incubation period was complete, 10 g of autoclaved HP-20 resin was added to each of the flasks under sterile conditions and the flasks were returned back to the incubator.

Extraction and Purification

The *Paenibacillus* sp. strain DE2SH fermentation broth (1.8 L) was filtered through a piece of glass wool under suction in a Buchner funnel to separate the supernatant from the mycelia. The supernatant was extracted with EtOAc and the mycelia and HP-20 resin were placed in a 1 L flask and extracted sequentially and alternatively with MeOH and CH₂Cl₂. All extracts were combined and evaporated under reduced pressure to obtain a total crude extract (4.24 g). The total crude extract was subjected to a modification of Kupchan's solvent partitioning process [25] that gave the four fractions FH (1.8 g), FD (1.1 g), FM (0.55 g), and WB (0.50 g). Phytochemical screening with Ninhydrin and Dragendorff on TLC plates followed by ¹H-NMR and HRESI-LC-MS showed that the FH contains isolable metabolites. Fraction FH was therefore subjected to semi-preparative HPLC separation and purification using a Phenomenex Luna C18 column (C18 250 × 10 mm, L × i.d.). Gradients of Solvent A: 20:80 (MeOH:H₂O) and Solvent B: 100% MeOH (100% A to 100% B in 30 min and hold for 30 min) were used as eluents with column flow rates set at 1.5 mL/min to afford compound **1** (1.3 mg/L, t_R = 37.5 min).

3.4. 1-Acetyl-2,4-dimethyl-3-phenethyl-1H-imidazol-3-ium (**1**)

Pale yellow oil substance; IR (neat) ν_{max}, 3095, 3074, 3062, 3028, 2872, 1710, 1661, 1621, 1435, 1496, 1374, 751, 703 cm⁻¹; UV (H₂O:MeOH) λ_{max} 210, 260, 309 nm (Supplementary Figure S2); for ¹H and ¹³C NMR data, see Table 1; Mass spectrometry data is detailed in Supplementary Figure S3.

3.5. Culture of Parasites and Mammalian Cell Lines

Blood stream forms of *Trypanosoma brucei* subsp. *brucei* strain GUTat 3.1 were cultivated in vitro to the logarithm phase using Hiram's Modified Iscove's Media (HMI9, Thermo Fisher Scientific) supplemented with 10% foetal bovine serum (Thermo Fisher Scientific) at 5% CO₂ and 37 °C. *Leishmania donovani* (Laveran and Mesnil) Ross (D10) was cultivated in vitro to the logarithm phase using Medium 199 (M199, Thermo Fisher Scientific) with 10% FBS at 5% CO₂ and 37 °C. Mouse macrophages (RAW 264.7 cell lines) were cultivated in vitro to the logarithm phase using Dulbecco's Modified Eagle Media (DMEM, Thermo Fisher Scientific) with 10% foetal bovine serum at 5% CO₂ and 37 °C [26].

3.6. Analysis of Cell Viability

For *Trypanosoma brucei* subsp. *brucei* strain GUTat 3.1 and *Leishmania donovani* (Laveran and Mesnil) Ross (D10), cells were seeded at a density of 3.0×10^5 cells/mL in 96 well plates at a two-fold dilution of the compound and incubated for 24 h. Alamar blue dye (resazurin, 10% V/V) was added to wells and incubated for another 24 h. For mouse macrophages (RAW 264.7), cell lines were plated at a density of 3.0×10^5 cells/mL for 48 h to allow for sufficient adherence to plates. The compound under investigation was then added to the cells in a two-fold dilution and incubated for another 24 h. Alamar blue dye (10% V/V) was added to wells and incubated for another 24 h. All experiments were run in quadruplicates. Spectrophotometric absorbance was recorded at a wavelength of 570 nm. Diminazene aceturate and amphotericin B were used as positive antitrypanosomal and antileishmanial control drugs respectively in the assays.

4. Conclusions

Paenidigamycin G (**1**) is one of the imidazole backbone alkaloids produced by the Ghanaian *Paenibacillus* sp. DE2SH (GenBank Accession Number: MH091697). This compound is always found in the hexane fraction-FH after the Kupchan solvent partitioning of crude extracts produced by liquid broth fermentation of the strain. Interestingly, among all the alkaloids isolated from DE2SH, **1** is the only compound produced in huge amounts when the strain is co-cultured with other microbes. The paenidigamycins showed potent antiparasitic biological activity profiles and hence, the conscious effort to evaluate the antiparasitic activity of **1** was made. However, **1** exhibited weak to moderate antileishmanial and antitrypanosomal activity when tested against *Leishmania donovani* (Laveran and Mesnil) Ross (D10) and *Trypanosoma brucei* subsp. *brucei* strain GUTat 3.1 with $IC_{50} = 115.41$ and $28.75 \mu\text{M}$, respectively. However, **1** displayed a promising selectivity profile towards *T. brucei* subsp. *brucei* due to its relatively low toxicity against normal mouse macrophages RAW 264.7 cells ($SI = 8.70$). The consistency of the production of **1** in liquid mono- and co-cultures presuppose some important biological functions which makes **1** a great candidate for further testing in order biological activity screens.

Supplementary Materials: The following are available online, Figure S1–S12: Spectrometry and Spectroscopy data.

Author Contributions: K.K. and H.D. collected mangrove sediments and isolated the strain DE2SH. A.S.C. and M.C. identified the exact taxonomy of the strain after K.K. isolated DNA and whole genome sequenced the strain. M.J. and H.D. provided access to facilities for mass spectrometry and data interpretation. K.K. performed chemical profiling to identify the major metabolites. S.K., G.M.T. and T.M. performed seed culture, large scale culture, isolation and purification of compound. K.K. measured all NMR, IR and UV, analyzed the results and integration of data to give the complete structure of the compound. K.K., S.K. and G.M.T. wrote the initial draft of the article which was edited and finalized by all the authors.

Funding: KK wishes to thank the Centre for African Wetlands (CAW), University of Ghana, for providing seed funding to enable the collection of soil samples for microbe isolation and a TWAS Research Grant Award_17-512 RG/CHE/AF/AC_G. K.K. is also very grateful to the Cambridge-Africa Partnership for Research Excellence (CAPREx), which is funded by the Carnegie Corporation of New York, for a Postdoctoral Fellowship. K.K. also appreciates the Cambridge-Africa ALBORADA Research Fund for support. K.K., H.D. and M.J. are grateful for this research which is jointly funded by the UK Medical Research Council (MRC) and the UK Department for International Development (DFID) under the MRC/DFID African Research Leaders Award (MR/S00520X/1). S.K. wishes to thank the Carnegie BANGA-Africa Project Award for a PhD scholarship and M.T. is grateful for an MPhil full scholarship from TWAS Research Grant Award_17-512 RG/CHE/AF/AC_G.

Acknowledgments: All the authors extend their gratitude to the Department of Chemistry, UG for providing NMR facility.

Conflicts of Interest: The authors declare no conflicts of interests.

References

1. De Vries, H.; Wagelmans, A.P.; Hasker, E.; Lumbala, C.; Lutumba, P.; De Vlas, S.J.; van de Klundert, J. Forecasting Human African Trypanosomiasis prevalences from population screening data using continuous time models. *PLoS Comput. Biol.* **2016**, *12*, e1005103. [[CrossRef](#)] [[PubMed](#)]
2. Copeland, N.K.; Aronson, N.E. Leishmaniasis: Treatment updates and clinical practice guidelines review. *Curr. Opin. Infect. Dis.* **2015**, *28*, 426–437. [[CrossRef](#)] [[PubMed](#)]
3. Colley, D.G.; Bustinduy, A.L.; Secor, W.E.; King, C.H. Human schistosomiasis. *Lancet* **2014**, *383*, 2253–2264. [[CrossRef](#)]
4. Rollinson, D.; Knopp, S.; Levitz, S.; Stothard, J.R.; Tchuente, L.A.T.; Garba, A.; Utzinger, J. Time to set the agenda for schistosomiasis elimination. *Acta Trop.* **2013**, *128*, 423–440. [[CrossRef](#)]
5. Burza, S.; Croft, S.L.; Boelaert, M. Leishmaniasis. *Lancet* **2018**, *392*, 951–970. [[CrossRef](#)]
6. Gaithuma, A.K.; Yamagishi, J.; Martinelli, A.; Hayashida, K.; Kawai, N.; Marsela, M.; Sugimoto, C. A single test approach for accurate and sensitive detection and taxonomic characterization of trypanosomes by comprehensive analysis of internal transcribed spacer 1 amplicons. *PLoS Negl. Trop. Dis.* **2019**, *13*, e0006842. [[CrossRef](#)]
7. Mitra, A.; Mawson, A. Neglected tropical diseases: Epidemiology and global burden. *Trop. Med. Infect. Dis.* **2017**, *2*, 36. [[CrossRef](#)]
8. Hotez, P.J.; Kamath, A. Neglected tropical diseases in sub-Saharan Africa: Review of their prevalence, distribution, and disease burden. *PLoS Negl. Trop. Dis.* **2009**, *3*, e412. [[CrossRef](#)]
9. Hotez, P.J.; Pecoul, B.; Rijal, S.; Boehme, C.; Aksoy, S.; Malecela, M.; Reeder, J.C. Eliminating the neglected tropical diseases: Translational science and new technologies. *PLoS Negl. Trop. Dis.* **2016**, *10*, e0003895. [[CrossRef](#)]
10. Pink, R.; Hudson, A.; Mouriès, M.A.; Bendig, M. Opportunities and challenges in antiparasitic drug discovery. *Nat. Rev. Drug Discov.* **2005**, *4*, 727–740. [[CrossRef](#)]
11. Cheuka, P.; Mayoka, G.; Mutai, P.; Chibale, K. The role of natural products in drug discovery and development against neglected tropical diseases. *Molecules* **2017**, *22*, 58. [[CrossRef](#)] [[PubMed](#)]
12. Addisu, A.; Adriaensen, W.; Balew, A.; Asfaw, M.; Diro, E.; Djirmay, A.G.; Adugna, A.H. Neglected tropical diseases and the sustainable development goals: An urgent call for action from the front line. *BMJ Glob Health.* **2019**, *4*, e001334. [[CrossRef](#)] [[PubMed](#)]
13. Gupta, K.G.; Kumar, V.; Kaur, K. Imidazole containing natural products as antimicrobial agents: A review. *Nat. Prod. J.* **2014**, *4*, 73–81. [[CrossRef](#)]
14. Sharma, A.; Kumar, V.; Kharb, R.; Kumar, S.; Sharma, C.P.; Pathak, P.D. Imidazole derivatives as potential therapeutic agents. *Curr. Pharm. Des.* **2016**, *22*, 3265–3301. [[CrossRef](#)]
15. Luca, L.D. Naturally occurring and synthetic imidazoles: Their chemistry and their biological activities. *Curr. Med. Chem.* **2006**, *13*, 1–23.
16. Liu, C.; Shi, C.; Mao, F.; Xu, Y.; Liu, J.; Wei, B.; Li, J. Discovery of new imidazole derivatives containing the 2,4-dienone motif with broad-spectrum antifungal and antibacterial activity. *Molecules* **2014**, *19*, 15653–15672. [[CrossRef](#)]
17. Li, X.; Zhan, P.; Clercq, D.E.; Liu, X. The HIV-1 non-nucleoside reverse transcriptase inhibitors (Part V*): Capravirine and its analogues. *Curr. Med. Chem.* **2012**, *19*, 6138–6149.
18. Zhang, W.; Shen, X.; Bergman, U.; Wang, Y.; Chen, Y.; Huang, M.; Deng, L. Drug utilisation 90%(DU90%) profiles of antibiotics in five Chinese children's hospitals (2002–2006). *Int. J. Antimicrob. Agents* **2008**, *32*, 250–255. [[CrossRef](#)]
19. Rotta, I.; Ziegelmann, P.K.; Otuki, M.F.; Riveros, B.S.; Bernardo, N.L.; Correr, C.J. Efficacy of topical antifungals in the treatment of dermatophytosis: A mixed-treatment comparison meta-analysis involving 14 treatments. *JAMA Dermatol.* **2013**, *149*, 341–349. [[CrossRef](#)]
20. Gaba, M.; Mohan, C. Development of drugs based on imidazole and benzimidazole bioactive heterocycles: Recent advances and future directions. *Med. Chem. Res.* **2016**, *25*, 173–210. [[CrossRef](#)]
21. Abdellatif, K.R.A.; Fadaly, W.A.A. New 1,2-diaryl-4-substituted-benzylidene-5-4H-imidazolone derivatives: Design, synthesis and biological evaluation as potential anti-inflammatory and analgesic agents. *Bioorg. Chem.* **2017**, *72*, 123–129. [[CrossRef](#)] [[PubMed](#)]

22. Acar, M.F.; Sari, S.; Dalkara, S. Synthesis, in vivo anticonvulsant testing, and molecular modeling studies of new nafimidone derivatives. *Drug Dev. Res.* **2019**, *80*, 606–616. [[CrossRef](#)] [[PubMed](#)]
23. Watts, A.E.; Maruyoshi, K.; Hughes, C.E.; Brown, S.P.; Harris, K.D. Combining the advantages of powder X-ray diffraction and NMR crystallography in structure determination of the pharmaceutical material cimetidine hydrochloride. *Cryst. Growth Des.* **2016**, *16*, 1798–1804. [[CrossRef](#)]
24. Osei, E.; Kwain, S.; Tetevi, M.G.; Anang, K.A.; Owusu, K.B.-A.; Camas, M.; Camas, A.S.; Ohashi, M.; Alexandru-Crivac, C.-N.; Deng, H.; et al. Paenidigamycin A, Potent Antiparasitic Imidazole Alkaloid from the Ghanaian *Paenibacillus* sp. DE2SH. *Mar. Drugs* **2019**, *17*, 9. [[CrossRef](#)]
25. Kwain, S.; Tetevi, G.M.; Mensah, T.; Camas, A.S.; Camas, M.; Dofuor, A.K.; Azerigyik, F.A.; Deng, H.; Jaspars, M.; Kyeremeh, K. Digyaindoleacid A: 2-(1-(4-Hydroxyphenyl)-3-oxobut-1-en-2-yloxy)-3-(1*H*-indol-3-yl) propanoic Acid, a Novel Indole Alkaloid. *Molbank* **2019**, *2019*, M1080. [[CrossRef](#)]
26. Yabu, Y.; Minagawa, N.; Kita, K.; Nagai, K.; Honma, M.; Sakajo, S.; Koide, T.; Ohta, N.; Yoshimoto, A. Oral and intraperitoneal treatment of *Trypanosoma brucei brucei* with a combination of ascofuranone and glycerol in mice. *Parasitol. Int.* **1998**, *47*, 131–137. [[CrossRef](#)]



© 2019 by the authors. Licensee MDPI, Basel, Switzerland. This article is an open access article distributed under the terms and conditions of the Creative Commons Attribution (CC BY) license (<http://creativecommons.org/licenses/by/4.0/>).